

See discussions, stats, and author profiles for this publication at: <https://www.researchgate.net/publication/50286459>

Complexity behind CO₂ capture on NH₂-MIL-53(Al)

ARTICLE in *LANGMUIR* · MARCH 2011

Impact Factor: 4.46 · DOI: 10.1021/la1045207 · Source: PubMed

CITATIONS

109

READS

167

9 AUTHORS, INCLUDING:



[Evgeny A Pidko](#)

Technische Universiteit Eindhoven

124 PUBLICATIONS 1,940 CITATIONS

SEE PROFILE



[Bert M Weckhuysen](#)

Utrecht University

595 PUBLICATIONS 16,731 CITATIONS

SEE PROFILE



[Joeri F M Denayer](#)

Vrije Universiteit Brussel

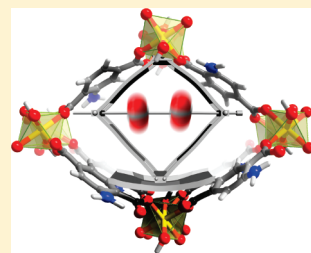
209 PUBLICATIONS 4,699 CITATIONS

SEE PROFILE

Complexity behind CO₂ Capture on NH₂-MIL-53(Al)Eli Stavitski,^{†,||} Evgeny A. Pidko,[‡] Sarah Couck,[§] Tom Remy,[§] Emiel J. M. Hensen,[‡] Bert M. Weckhuysen,^{||} Joeri Denayer,[§] Jorge Gascon,^{†,*} and Freek Kapteijn[†][†]Catalysis Engineering - ChemE, Delft University of Technology, Julianalaan 136, 2628 BL Delft, The Netherlands.[‡]Schuit Institute of Catalysis, Department of Chemistry and Chemical Engineering, Eindhoven University of Technology, P.O. Box 513, 5600 MB Eindhoven, The Netherlands[§]Department of Chemical Engineering, Vrije Universiteit Brussel, Belgium^{||}Inorganic Chemistry and Catalysis Group, Department of Chemistry, Utrecht University, Sorbonnelaan 16, 3584 CA Utrecht, The Netherlands

Supporting Information

ABSTRACT: Some Metal Organic Frameworks (MOFs) show excellent performance in extracting carbon dioxide from different gas mixtures. The origin of their enhanced separation ability is not clear yet. Herein, we present a combined experimental and theoretical study of the amino-functionalized MIL-53(Al) to elucidate the mechanism behind its unusual high efficiency in CO₂ capture. Spectroscopic and DFT studies point out only an indirect role of amine moieties. In contrast to other amino-functionalized CO₂ sorbents, no chemical bond between CO₂ and the NH₂ groups of the structure is formed. We demonstrate that the functionalization modulates the “breathing” behavior of the material, that is, the flexibility of the framework and its capacity to alter the structure upon the introduction of specific adsorbates. The absence of strong chemical interactions with CO₂ is of high importance for the overall performance of the adsorbent, since full regeneration can be achieved within minutes under very mild conditions, demonstrating the high potential of this type of adsorbents for PSA like systems.



INTRODUCTION

The growing concern about the harmful effect of greenhouse gases emissions on the world's climate stirs scientific and technological interest in carbon dioxide sequestration. Research and development efforts into CO₂ capture and sequestration technologies are essential to allow mankind to continue using fossil fuels until renewable alternatives have been developed at a reasonable economical cost.¹ The scientific and societal importance of research into the area of CO₂ separation and its possible industrial application is therefore beyond discussions.

One of the industrially established methods of CO₂ capture is liquid-phase absorption. Commercial large-scale processes aimed at CO₂ removal from gas streams usually employ basic aqueous solutions of alcoholic amines, e.g. mono- and triethanolamine.¹ A drawback of this approach is the contamination of the gas with solvent vapors and degradation of the amines due to the high temperature treatments required to regenerate the absorbent. To prevent this, task specific ionic liquids, which exhibit extremely low partial pressures up to ~300 °C, have been designed as solvents or active absorbents.² However, the tendency of the frequently used phosphine anions to decompose via Beckman rearrangement at moderate temperatures³ limits their use. An alternative route involves utilization of functionalized porous materials as CO₂ adsorbents. Mesoporous silica materials functionalized with different amines have been proven to be an attractive approach for manufacturing high performance CO₂ sorbents.^{4,5} These porous solids show an excellent affinity toward

CO₂, although their regeneration represents a technical challenge.

Along these lines, we endeavored to combine the amine separation activity and the properties of metal-organic frameworks (MOFs). In recent years, the combination of organic and inorganic subunits in fully crystalline porous materials has given rise to thousands of MOF structures with a vast chemical versatility.⁶ A special class of MOFs consists of those that can reversibly alter their framework structure when guest molecules are introduced.⁷ This results in special properties like the breathing effect⁸ and the gate phenomenon,^{9,10} where pores contract or open upon adsorption. An example of a breathing material is MIL-53 and its functionalized derivatives.^{8,11–14} MIL-53 is built from MO₄(OH)₂ octahedra (where M can be Fe³⁺, Cr³⁺, Al³⁺ or Ga³⁺) and 1,4-benzenedicarboxylate (terephthalate) linkers. In this way a crystalline material with 1-D diamond shaped pores is formed. With the discovery of MOFs, it was only a matter of time until the combination of amines and flexibility was proposed for CO₂ capture. Recently, we reported the excellent performance of the NH₂-MIL-53(Al) in the separation of CO₂ from CH₄.¹⁵ NH₂-MIL-53(Al)^{16,17} is a material based on the topology of MIL-53. During the synthesis of amino-MIL-53(Al), 2-amino terephthalic acid replaces terephthalic acid as linker molecule.

Received: November 13, 2010

Revised: January 18, 2011

Published: March 04, 2011

In comparison with other porous amino functionalized materials, MOFs offer several advantages, such as higher specific surface areas and a higher concentration of monodispersed functionalities. This resulted in an excellent selectivity and an impressive sorption capacity toward CO₂. Since then, several groups have reported on amino-modified MOFs for similar purposes.^{18,19} However, very little is known about the physics and chemistry behind the improved performance and even less about long-term utilization and regeneration of these materials.

Here we present a combined spectroscopic, theoretical (DFT) and performance investigation that demonstrates the high separation efficiency and regeneration capacity of the NH₂-MIL-53(Al) for the separation of CO₂ from mixtures with different gases and moisture. We established that amino-groups are only indirectly responsible for the improved separation performance. In contrast to other amino-modified materials, no chemical bond between CO₂ and the amine groups of the structure is formed, but the interplay of weak dispersion forces control the performance.

EXPERIMENTAL SECTION

Synthesis. All chemicals were obtained from Sigma-Aldrich and were used without further purification. NH₂-MIL-53(Al) was synthesized using the method described elsewhere.¹⁶ 2.10 mmol aluminum nitrate nonahydrate dissolved in 15 mL DMF and 3.12 mmol 2-amino-terephthalic acid dissolved in 15 mL DMF were mixed in a Teflon insert and placed in an autoclave. The autoclave was kept at 150 °C for 3 days. The yellow gel product was filtered off and washed with acetone. After acetone removal, the product was washed overnight with boiling methanol under reflux and dried at 110 °C in vacuum for 8 h.

DRIFTS. DRIFT spectra were recorded in a Thermo Nicolet Nexus FTIR spectrometer equipped with a high-temperature, high-pressure cell with ZnSe windows. Before collecting the spectra the different samples were pretreated in a pure helium flow at 250 °C for 30 min. KBr was used as background. A flow of CO₂ (purity of 99.995%) at 10 mL/min was maintained during the high-pressure measurements.

Adsorption & Separation Experiments. Adsorption isotherms of pure CO₂ (purity of 99.995%), CH₄ (purity of 99.95%), N₂ (purity of 99.995%), and H₂ (purity of 99.995%) were determined using the volumetric technique with an apparatus from VTI (HPA 100). About 0.5 g of amino-MIL-53(Al) sample was loaded in the sample container. Before every measurement, the adsorbent was regenerated by raising the temperature to 250 °C at a rate of 1 °C/min under vacuum (10^{−7} mbar). The studied experimental pressure ranged from 0.02 to 30 bar.

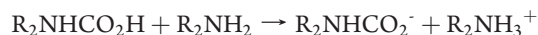
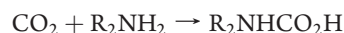
The separation of gas mixtures with NH₂-MIL-53 was studied by performing breakthrough experiments. A column with a length of 30 cm and an internal diameter of 0.216 cm was packed with 600 mg of NH₂-MIL-53(Al) pellets. Pellets were obtained by pressing the powder to a solid disk, crushing the disk followed by sieving to the desired fraction of 500 – 630 μm. Prior to the measurements, the adsorbent was regenerated *in situ* by flowing pure He through the column and raising the temperature to 150 °C at a rate of 5 °C/min and keeping this temperature for 20 min. The separation of mixtures of CO₂ and other gases (N₂, H₂, CH₄) was studied at 30 °C and various gas compositions at flow ranges from 0.36 to 0.80 mmol/min. The breakthrough profiles show the volumetric flow rate of the components of the mixture at the outlet of the column normalized to their feed flow rate as a function of time.

Computational Details. All quantum chemical calculations were carried out within density functional theory (DFT) with the gradient-corrected Perdew-Burke-Ernzerhofer (PBE)²⁰ exchange-correlation functional using a combination of Vienna Ab Initio Simulation Package

(VASP)²¹ and CPMD²² programs. The thermodynamic properties discussed in the manuscript were corrected for van der Waals interactions following the PBE+Dispersion (DFT+D, PBE+D) approach (see Supporting Information for further computational details).

RESULTS AND DISCUSSION

Conventionally, CO₂ capture by solvated amines and amino-functionalized ionic liquids is attributed to carbamate formation, which is instantaneously followed by the reaction with a second amine molecule, producing a zwitterion:²³



Therefore, two moles of amine are required to capture one mol of CO₂. The above scheme is valid for dry conditions. Formation of carbamates leads to long-term deactivation of the adsorbent,²⁴ which could be circumvented by adding moisture to the gas stream. In this case bicarbonates are formed upon absorption, allowing for faster regeneration but at still relatively high temperatures. On the contrary, CO₂ adsorption on adsorbents, such as zeolites or activated carbons, is inhibited by moisture.²⁵ In the case of amines grafted on porous supports, such as (aminopropyl)triethoxysilane on SBA-15, carbonate, bicarbonate and carbamic acid were detected by IR spectroscopy.²⁶ In accordance with the schemes above, we attributed the enhanced performance of the NH₂-MIL-53(Al) to the direct interaction of amines with CO₂.¹⁵ However, we anticipated that van der Waals interactions contribute to the adsorption.²⁷ To unveil the nature of the interaction between the MOF and CO₂ we followed the adsorption process with Diffuse-Reflectance Infrared Fourier Transform spectroscopy (DRIFTS) up to much higher CO₂ pressures. Prior to the experiments the sample was activated at 250 °C to remove physisorbed water.

Several features in the DRIFT spectrum, shown in Figure 1 of the activated sample, require closer inspection. A broad band centered around 3680 cm^{−1} could be assigned to the bridging hydroxyl group of the MIL-53, i.e. Al–OH–Al.²⁸ The band position is very close to that reported for unfunctionalized MIL-53, although the relative intensity of this band is much lower. The broad band between 3500 and 2500 cm^{−1} may originate from the hydroxyl groups, which are directly interacting with the neighboring amines (see below). Two sharp bands at 3393 and 3505 cm^{−1} in the spectra are due to symmetric and asymmetric vibrations of NH₂ groups, respectively. Positions of the N–H stretching bands are characteristic for the type of the hydrocarbon moiety to which the amine group is bound. For example, in the case of aniline these bands appear at ~3421 and 3508 cm^{−1}.²⁹ Another factor affecting the position of the bands is intra- or intermolecular hydrogen bonding involving the NH₂. Unlike hydroxyl groups, whose bands are red-shifted upon hydrogen bonding, the situation is more complex in the case of amines. Intramolecular interaction of one of the two hydrogen atoms lifts the degeneracy of the two N–H local oscillators resulting in frequency reduction for one of the modes. This leads to the larger red shift of the symmetric band compared to that of the asymmetric one, increasing the splitting between the two bands. However, due to the low proton-donating ability of the amino group, as well as its nonplanar geometry, hydrogen bonding in the ortho-substituted anilines was found to be very weak.³⁰ In the present case, a red shift by 28 cm^{−1} of the symmetric band and a 34 cm^{−1} blue shift of the asymmetric band,

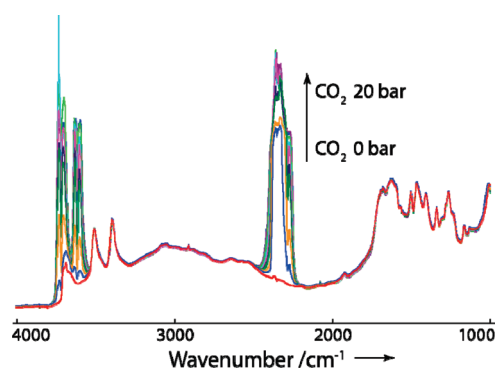


Figure 1. DRIFTS spectra of the $\text{NH}_2\text{-MIL-53(Al)}$ upon CO_2 adsorption at 25 °C.

with respect to aniline³¹ are found. The shifts are identical to those obtained for anthranilic acid, as well as for the aminoterephthalic acid linker,³² indicating that the interaction with other constituents of the framework does not considerably affect the vibrational properties of NH_2 groups.

To unveil the specific $\text{NH}_2\text{-CO}_2$ interactions, the amine region ($3300\text{--}3600\text{ cm}^{-1}$) of these DRIFT spectra is expanded in Figure 2. One should note that the N-H stretching region is only slightly affected upon CO_2 exposure. The latter result is quite surprising, since it is in contrast to the previous published results on amino-functionalized materials. For example, Zhang et al. reports absorption of CO_2 by tetrabutylphosphonium amino acid ionic liquids.³³ Upon exposure, the NH_2 doublet disappears, giving rise to a band at 3234 cm^{-1} , which was assigned to the perturbed N-H stretching vibration in the carbamate. CO_2^- species in the zwitter-ion structure give rise to the band at $\sim 1660\text{ cm}^{-1}$. A similar suppression of the $3370\text{--}3300\text{ cm}^{-1}$ doublet has been observed for an amine-bearing porous silicon film.³⁴ Upon removal of preadsorbed CO_2 from amino-SBA-15 the NH_2 band at 3372 cm^{-1} was recovered.²⁶ This, along with the absence of significant changes in the fingerprint region, indicates that the formation of a chemical bond between the amine groups and CO_2 is unlikely.

In the difference spectra (using the bare $\text{NH}_2\text{-MIL-53}$ as background) (Figure 2b) a slight decrease of the N-H stretching bands is observed. This intensity change amounts to only ca. 5% of the overall intensity. The negative contributions are narrower than the original bands and at the high wavenumber side of the N-H stretching vibrations, indicating that only a specific type of the amino groups, most likely on the external surface, undergoes strong interaction with the adsorbed molecules. It is easy to figure out that amine groups at the external surface are not in a confined environment, making the interaction with CO_2 more likely. Unfortunately, changes in the hydroxyl region of the DRIFTS spectra taken at high CO_2 pressures could not be detected because of the overlapping strong gas-phase CO_2 bands. Therefore, only spectra at low pressures could be analyzed. The spectra recorded in transmission mode at pressures up to 30 mbar, given in the Supporting Information (Figure S1), do not show strong perturbations in the spectra of bridging OH groups either.

In view of the striking IR results, periodic dispersion-corrected plane-wave density functional theory (DFT+D) calculations were performed to unravel the molecular phenomena underlying the enhanced selectivity of CO_2 adsorption on the $\text{NH}_2\text{-MIL-53(Al)}$. Such atomistic simulations allow a more profound

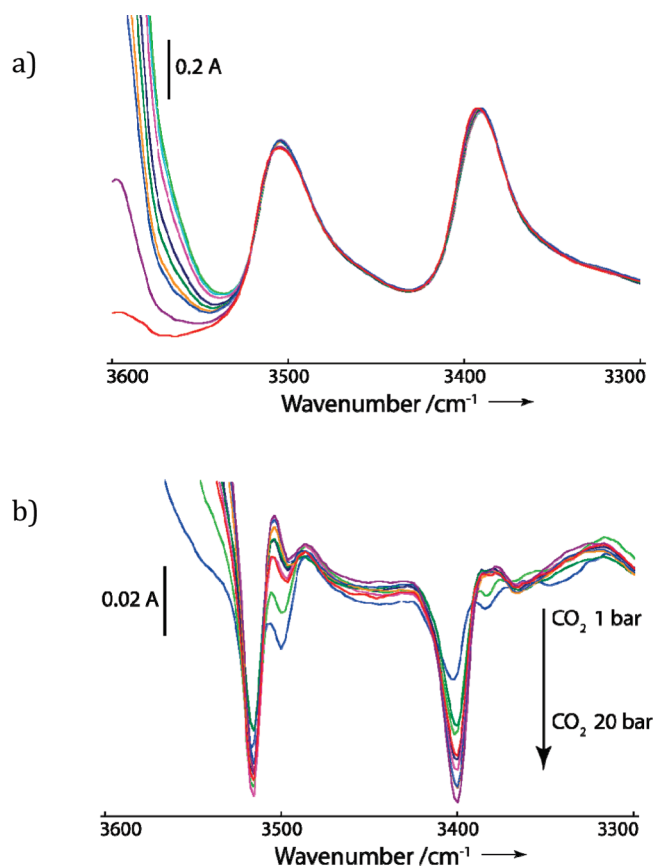


Figure 2. $3300\text{--}3600\text{ cm}^{-1}$ region of the DRIFTS spectra of the $\text{NH}_2\text{-MIL-53}$ upon CO_2 adsorption (a) and difference spectra (b) at 25 °C.

insight into the structural and chemical properties of the materials, as well as a direct monitoring of interatomic arrangements in the vicinity of asymmetric building blocks. In DFT simulations the distribution of atoms is set explicitly. This methodological advantage is at the same time a serious drawback: only a limited number of potential isomeric structures with different conformations and relative orientation of asymmetric linkers can be analyzed computationally. Because of these limitations the DFT results presented here are intended to assist the molecular level interpretation of the spectroscopic and adsorption data rather than to give a direct quantitative comparison with the experiment.

In a first step, the effect of the functionalization on the configuration of the empty framework was studied. Both the parent MIL-53(Al) and the amino-modified $\text{NH}_2\text{-MIL-53(Al)}$ were considered. According to our calculations, in the absence of adsorbates, the open form *-large pore-* of unfunctionalized ($\text{MIL-53}^{\text{lp}}$) material, represented by an orthogonal unit cell, is energetically preferred over the monoclinic *-narrow pore-* ($\text{MIL-53}^{\text{np}}$) polymorph, by only 3 kJ mol^{-1} . The opposite situation is predicted for the case of the amino-modified MIL-53 , for which the *np* structure is favored by 14 kJ mol^{-1} compared to the *lp* one. Both observations agree with temperature-programmed XRD analyses^{11,35} for these structures (Figure 3). The preference for the contracted structure ($\text{NH}_2\text{-MIL-53}^{\text{np}}$) is due to more efficient hydrogen bonding involving the NH_2 moieties and the $[\text{AlO}_6]_\infty$. This is evident from the differences in the corresponding optimized interatomic distances realized in the two polymorphs of $\text{NH}_2\text{-MIL-53(Al)}$ (Figure 4).

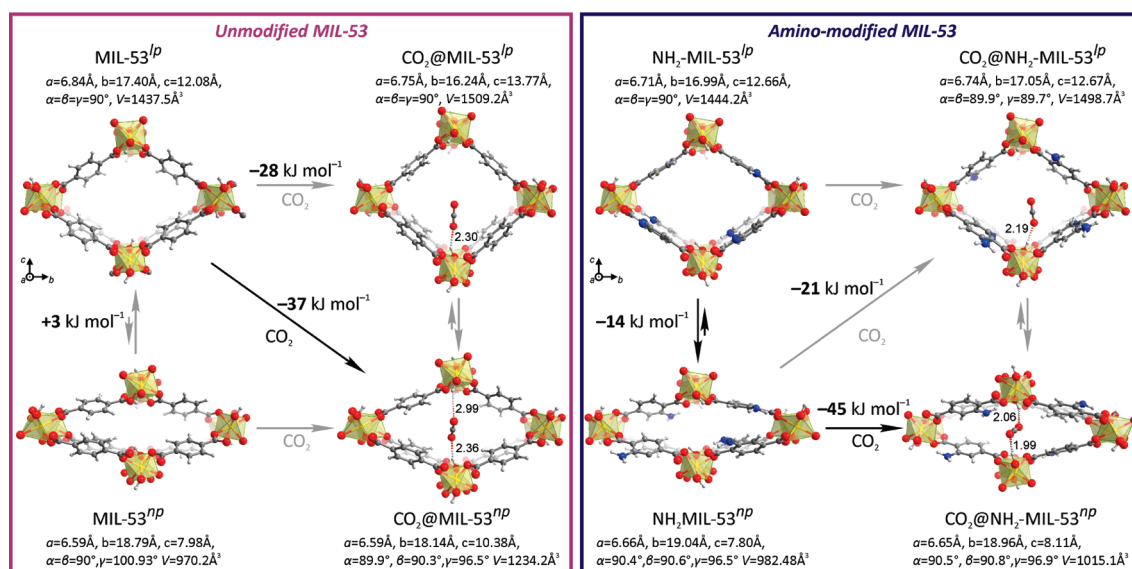


Figure 3. Optimized structures and relative energies of (left) parent MIL-53 and (right) amino-functionalized NH_2 -MIL-53 materials and their complexes with CO_2 .

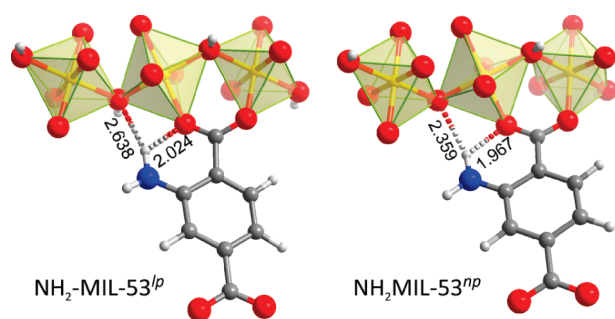


Figure 4. Selected intermolecular $-\text{NH}_2 \cdots [\text{AlO}_6]_\infty$ contacts (distances are in Å) observed in the optimized NH_2 -MIL-53^{lp} and NH_2 -MIL-53^{np} structures.

The contraction of the orthogonal MIL-53 lattice induces substantial geometrical distortions. Energy losses associated with such unfavorable perturbations are then partially compensated by the formation of additional intermolecular interactions that can only be realized within the np structure. In the case of the parent MIL-53 material, the formation of the monoclinic polymorph results in the formation of van der Waals interactions between the terephthalate joints. The optimized MIL-53^{np} model exhibits a uniform array of intermolecular $\text{CH} \cdots \pi$ contacts within the MOF channels. Nevertheless, the very low strength of such individual interactions and their noncooperative behavior is insufficient for an efficient stabilization of the contracted MIL-53 polymorph. The much more pronounced energy difference between the two polymorphs estimated for the case of the amino-modified material is due to the stronger hydrogen-bonding interactions determining the preferred structure compared to the van der Waals interaction dominating the structure of the unsubstituted MIL-53. Very recently, Walker et al.³⁶ reported a DFT+D study on the stability of different MIL-53 polymorphs, who predicted an ~ 10 kJ/mol higher stability of the np structure. The results from Walker and co-workers are in good agreement with neutron diffraction experiments presented by Liu et al.¹² The authors reported that MIL-53(Al) can be

converted to the np form by only decreasing temperature and without the aid of any guest molecules. Later, Mendt et al.³⁷ using electron spin resonance spectroscopy (ESR) to monitor the same evolution with temperature showed that indeed the dehydrated MIL-53(Al) transforms from its lp into the np phase between 150 and 60 K, while the back transformation from the np to the lp phase occurs at considerably higher temperatures, between 330 and 375 K, indicating a large thermal hysteresis. However, the phase transformation of the material is not complete. In contrast to the claims of Walker et al.³⁶ and Liu et al.,¹² a fraction of up to 20% of the material does not undergo the lp to np phase transition and remains in its lp phase even at temperatures as low as 8 K. This suggests very small differences in energy between the np and the lp forms, in line with our computational results.

The larger stabilization than in our calculations reported by Walker et al.³⁴ could arise from the increased errors due to the superposition of localized Gaussian-type basis sets of the adjacent aromatic ligands. The plane wave DFT methodology used in the current study is inherently free from the basis set superposition error. The very minor energetic effects within this dispersion-dominated system cannot be quantitatively described within the semiempirical DFT+D formalism. In fact, Walker et al.³⁶ reported a ΔS value for the lp \rightarrow np transition of $0.0138 \text{ kJ mol}^{-1} \text{ K}^{-1}$ that in combination with the respective transition enthalpy of $-8.43 \text{ kJ mol}^{-1}$ indicates that the transition between the lp and np polymorphs is reached only above 600 K (200 K higher than in reality^{12,37}). We conclude therefore that the temperature-induced structural transition of MIL-53 should be further explored using a range of theoretical methodologies including the fully ab initio methods recently proposed by Sauer and co-workers as a quantitative tool for the description of various dispersion-dominated phenomena in zeolite-based materials.³⁸

Notwithstanding that this temperature-induced structural transition is not the focus of the present study, considering that it is generally accepted that the accuracy of standard DFT methodologies is ca. 10 kJ/mol, the substantial qualitative differences observed between the behavior of MIL-53 and

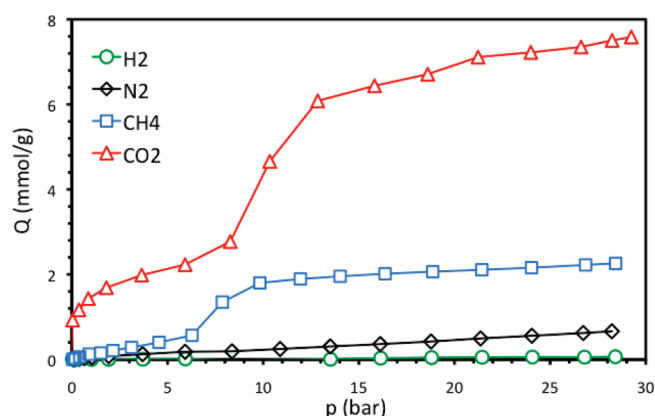


Figure 5. (a) Adsorption isotherms of H₂, N₂, CH₄, and CO₂ at 10 °C on NH₂-MIL-53(Al).

NH₂-MIL-53 materials cannot be rationalized solely by the deficiencies of the computational methodology used.

Despite the modification of the organic linkers with NH₂ moieties, which breaks the CH $\cdots\pi$ interaction network, a wide variety of van der Waals contacts between the organic structural fragments is evident in the optimized NH₂-MIL-53^{np} structure. More important is the enhancement of the $-\text{NH}_2\cdots[\text{AlO}_6]_\infty$ hydrogen bonding interactions noted above (Figure 4). Besides the direct stabilizing effect, this may have a considerable impact on the flexibility of the aluminum-occupied oxygen octahedra associated with the decreased basicity of the hydrogen-bonded carboxylic groups and bridging OH ligands. The resulting increased local flexibility of the $[\text{AlO}_6]_\infty$ chains reduces the energy losses associated with the structural perturbations upon formation of the np structure. The combination of these factors leads to the higher relative stability of NH₂-MIL-53(Al)^{np}.

The flexibility of the MIL-53 network is still a matter of discussion. Removal of guest molecules, such as linker or solvent by heating, leads to either an expansion (in case of Al, Ga, and Cr) or a contraction of the cell (in case of Fe).²⁸ Several attempts to rationalize the breathing dynamics of these frameworks have been published. All these reports are based on experimental observations or fitting of experimental data, from which no molecular insight can be derived.^{8,11–13,28,39} Here, we can rationalize the breathing of the framework based on the atomistic DFT simulations. On the basis of the optimized structures for both frameworks, the interactions underlying the CO₂ adsorption were investigated by the DFT+D method. In agreement with previous studies,^{40–43} adsorption of carbon dioxide on MIL-53 is directed by the formation of rather weak hydrogen bonds between CO₂ and bridging hydroxyl groups of the lattice (Figure 3). The CO₂ complexes formed on each of the adsorbents show very similar bonding patterns, but with a remarkable difference in the orientation inside the framework. Similar results were reported very recently by Torrisi et al.,^{44–46} but these authors only studied either the linkers or the lp form of the MIL-53 isomers at very low CO₂ loadings, while for both materials, the formation of closed structures is favored at these conditions (Figure 3). Confinement of the CO₂ molecule within the np MIL-53(Al) and np NH₂-MIL-53(Al) structures allows bidentate coordination of the adsorbent to the bridging OH groups located at the opposite sides of the channel. In line with the DRIFTS results, no direct strong interaction between the adsorbed molecules and the amino groups are observed. In

principle, an elongated (>2.9 Å) intermolecular O₂C \cdots NH₂ contact can be present within the adsorption complexes in the lp NH₂-MIL-53 structure with specific arrangement of NH₂ moieties, but such interactions contribute no more than 2 kJ mol^{−1} and would only appear at high loadings, when the lp structure is formed. Therefore, this interaction is not expected to cause any significant effect in the DRIFT spectra.⁴⁶ Indeed, our calculations indicate a negligible stability difference between the adsorption complexes in which an additional interaction with the basic NH₂ moiety is present, and those governed solely by the interaction with the bridging OH groups (Supporting Information Figure S11).

The presence of the basic amino groups in the framework influences the intrinsic properties of the CO₂ adsorption sites. A comparison of the OH \cdots O=C=O distances in the optimized structures (Figure 3) reveals the formation of shorter hydrogen bonds in the amino-modified material. This effect is most likely associated with the increased acidity of the bridging OH groups due to the interaction of the adjacent $[\text{AlO}_6]$ units with the $-\text{NH}_2$ moieties. Also, in this case such elongated H \cdots O contacts as those observed in the adsorption complexes considered are usually weak. Their individual contribution to the overall adsorption energy is expected not to exceed 5–10 kJ mol^{−1}.^{47,48} Similar cooperative effects have been recently suggested for other amine containing MOFs.⁴⁹

With this information in mind, the single component adsorptive properties of the NH₂-MIL-53(Al) were revisited. Adsorption isotherms of pure CO₂, CH₄, N₂, and H₂ were determined at different temperatures between 0.02 and 30 bar. Results at 10 °C are plotted in Figure 5. As expected at the studied temperatures, H₂ is not adsorbed in the experimental pressure range. Remarkably, and in contrast to results reported for the unfunctionalized MIL-53(Al), N₂ is only adsorbed in small amounts at pressures above 2 bar, while CH₄ is not adsorbed at all below 1 bar. A discontinuity in the methane isotherm is observed between 6 and 10 bar, while CO₂ shows a two-step profile as was already observed before on MIL-53. The whole set of results can be explained considering the energy schemes drawn in Figure 3. The main difference between both frameworks resides in the contraction after solvent removal in the preparation. The unfunctionalized material in the lp form allows methane to enter the pores. Since there is hardly any interaction between the nearly apolar hydrocarbon and the pores, no structural transition is found through adsorption, resulting in an regular type I isotherm (see Supporting Information Figure S4).^{40,50} In contrast, adsorption of CO₂ induces the transition from the large to the narrow pore form. In the case of the NH₂-MIL-53(Al), after solvent removal, the framework is already in the narrow pore form; therefore, CO₂ adsorption only produces minor changes in the structure at low pressures, while due to the above-mentioned NH₂–OH interaction, a higher partial pressure (10 bar) is needed to fully open the framework. In contrast, both methane and nitrogen adsorption, with their larger kinetic diameter and weaker energetic interaction with the framework as compared to CO₂, are excluded until their pressure is large enough to drive the adsorption. At lower temperature (see Supporting Information Figure S2), a second step in the CH₄ isotherm is observed at even higher pressure (>20 bar). This corresponds to the real transition of the framework, from the np to the lp form.

With this knowledge in hand, we are now able to identify the specific phenomena that strongly determine the performance of the material. The high CO₂ adsorption ideal selectivity (almost infinite) is driven by the preference for the formation of the

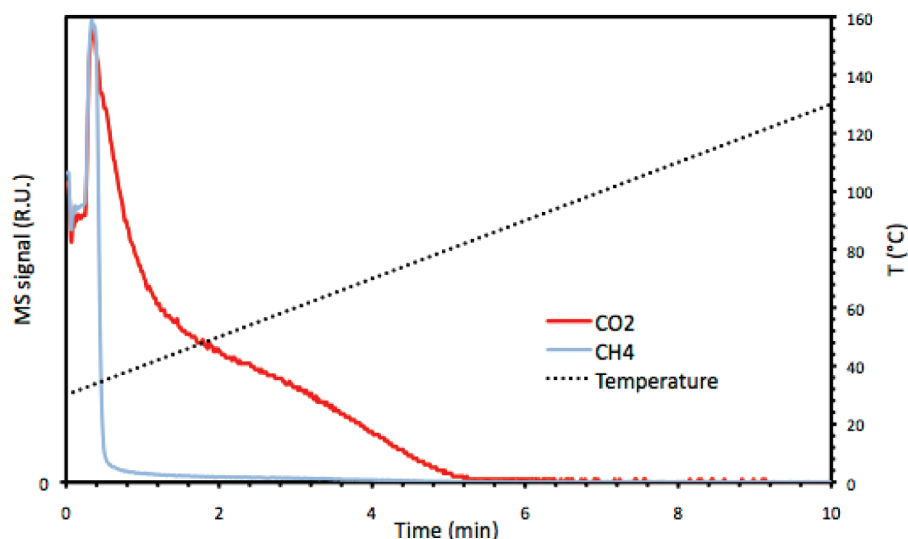


Figure 6. Desorption profiles of CH₄ and CO₂ from a NH₂-MIL-53 column during heating from 30 to 130 °C under continuous He flow.

narrow pore polymorph after the solvent removal. On the other hand, a rather facile opening of the MIL-53 structure is needed to accommodate larger quantities of carbon dioxide. In the case of NH₂-MIL-53(Al), the associated energy losses are substantial. The flexibility of coordination polyhedra around the metal centers should be enhanced to ensure a smoother increase of the pore size upon the increasing CO₂ pressure and thus allow for a larger CO₂ adsorption capacity. One expects that such a behavior can be induced by variation of the metal centers or by introduction of a proper functional group in the aromatic linker.

This induced-fit type pore⁵¹ behavior has very important consequences for separation, since the NH₂-MIL-53(Al) can be used as a powerful shape selective adsorbent: starting from a np form allows it to efficiently accommodate adsorbed molecules of a certain size while hampering the adsorption of bigger molecules. In addition, by reducing the pore size, an increase in the enthalpy of adsorption is expected.⁵² In fact, breakthrough experiments performed with different gas mixtures (see Supporting Information) demonstrate that CO₂ is selectively retained by the adsorbent, while H₂, N₂, and CH₄ are nearly not adsorbed, which leads to their immediate elution from the adsorption column, resulting in very high mixture separation factors (as high as 75 for low CO₂ partial pressures), even in the presence of moisture (Supporting Information Figure S9) and at very low CO₂ concentrations (Supporting Information Figure S8).

The absence of strong chemical interactions with CO₂ also plays in favor of the amino functionalized framework. For practical purposes, regeneration of the adsorbent is an important aspect as it determines a large part of the operational cost of the adsorptive separation process. Supporting Information Figure S11 shows the desorption profile measured at the outlet of the adsorption column presaturated with a mixture of CO₂ and CH₄. The column was flushed with He (0.8 mmol/min) and kept at a constant temperature of 30 °C. The concentration of the very weakly adsorbed CH₄ drops almost immediately to zero, but also CO₂ is desorbed in less than 15 min. At elevated temperature, the regeneration is further accelerated. In contrast to other adsorbents and to liquid absorption, a temperature of only 80 °C is sufficient to remove all CO₂ from the material (Figure 6), again in line with the IR and DFT observations.

Compared to the state of the art adsorbents for the separation of CO₂,^{53,54} the NH₂-MIL-53(Al) framework shows a higher ideal selectivity and higher separation factors. These features combined with an acceptable CO₂ loading and a fast regenerability demonstrate the high potential of this adsorbent.

CONCLUSIONS

The enhanced performance of the NH₂-MIL-53(Al) framework in CO₂ capture and separation is due to its specific flexibility. The adsorption properties and separation ability of the NH₂-MIL-53(Al) are mostly due to a delicate interplay of weak dispersion forces controlling the flexibility of the framework. The stable np starting form allows it to efficiently accommodate adsorbed molecules of a certain size while hampering the adsorption of bigger molecules (induced fit type pore). In contrast to other amino-functionalized materials, the intrinsic chemical properties of the amine adsorption sites are of lower importance. The role of the basic amine functionality in the framework on the adsorption properties is only indirect. The absence of strong chemical interactions with CO₂ is of high importance for the overall performance of the adsorbent, since full regeneration can be achieved within minutes under very mild conditions, demonstrating the high potential of this type of adsorbents for PSA-like systems.

ASSOCIATED CONTENT

S Supporting Information. Additional information as described in the text. This material is available free of charge via the Internet at <http://pubs.acs.org>.

AUTHOR INFORMATION

Corresponding Author

*j.gascon@tudelft.nl.

ACKNOWLEDGMENT

E.S., E.A.P., and J.G. gratefully acknowledge The Netherlands National Science Foundation (NWO) for their personal VENI

grants. NWO-NCF is acknowledged for access to computing facilities.

REFERENCES

- (1) Tagliabue, M.; Farrusseng, D.; Valencia, S.; Aguado, S.; Ravon, U.; Rizzo, C.; Corma, A.; Mirodatos, C. *Chem. Eng. J.* **2009**, *155*, 553.
- (2) Bates, E. D.; Mayton, R. D.; Ntai, I.; Davis, J. H. *J. Am. Chem. Soc.* **2002**, *124*, 926.
- (3) Nikitin, E. V.; Romakhin, A. S.; Zagumenov, V. A.; Babkin, Y. A. *Electrochim. Acta* **1997**, *42*, 2217.
- (4) Tang, Y. D.; Landskron, K. *J. Phys. Chem. C* **2010**, *114*, 2494.
- (5) Belmabkhout, Y.; De Weireld, G.; Sayari, A. *Langmuir* **2009**, *25*, 13275.
- (6) Long, J. R.; Yaghi, O. M. *Chem. Soc. Rev.* **2009**, *38*, 1213.
- (7) Ferey, G.; Serre, C. *Chem. Soc. Rev.* **2009**, *38*, 1380.
- (8) Serre, C.; Millange, F.; Thouvenot, C.; Nogues, M.; Marsolier, G.; Louer, D.; Ferey, G. *J. Am. Chem. Soc.* **2002**, *124*, 13519.
- (9) Noro, S.; Tanaka, D.; Sakamoto, H.; Shimomura, S.; Kitagawa, S.; Takeda, S.; Uemura, K.; Kita, H.; Akutagawa, T.; Nakamura, T. *Chem. Mater.* **2009**, *21*, 3346.
- (10) Seo, J.; Matsuda, R.; Sakamoto, H.; Bonneau, C.; Kitagawa, S. *J. Am. Chem. Soc.* **2009**, *131*, 12792.
- (11) Loiseau, T.; Serre, C.; Huguenard, C.; Fink, G.; Taulelle, F.; Henry, M.; Bataille, T.; Ferey, G. *Chem.—Eur. J.* **2004**, *10*, 1373.
- (12) Liu, Y.; Her, J. H.; Dailly, A.; Ramirez-Cuesta, A. J.; Neumann, D. A.; Brown, C. M. *J. Am. Chem. Soc.* **2008**, *130*, 11813.
- (13) Millange, F.; Guillou, N.; Walton, R. I.; Greneche, J. M.; Margiolaki, I.; Ferey, G. *Chem. Commun.* **2008**, 4732.
- (14) Hamon, L.; Llewellyn, P. L.; Devic, T.; Ghoufi, A.; Clet, G.; Guillermin, V.; Pirngruber, G. D.; Maurin, G.; Serre, C.; Driver, G.; van Beek, W.; Jolimaite, E.; Vimont, A.; Daturi, M.; Ferey, G. *J. Am. Chem. Soc.* **2009**, *131*, 17490.
- (15) Couck, S.; Denayer, J. F. M.; Baron, G. V.; Remy, T.; Gascon, J.; Kapteijn, F. *J. Am. Chem. Soc.* **2009**, *131*, 6326.
- (16) Gascon, J.; Aktay, U.; Hernandez-Alonso, M. D.; van Klink, G. P. M.; Kapteijn, F. *Catal.* **2009**, *261*, 75.
- (17) Ahnfeldt, T.; Guillou, N.; Gunzelmann, D.; Margiolaki, I.; Loiseau, T.; Ferey, G.; Senker, J.; Stock, N. *Angew. Chem., Int. Ed.* **2009**, *48*, 5163.
- (18) Vaidhyanathan, R.; Iremonger, S. S.; Dawson, K. W.; Shimizu, G. K. H. *Chem. Commun.* **2009**, 5230.
- (19) An, J.; Geib, S. J.; Rosi, N. L. *J. Am. Chem. Soc.* **2010**, *132*, 38.
- (20) Perdew, J. P.; Burke, K.; Ernzerhof, M. *Phys. Rev. Lett.* **1996**, *77*, 3865.
- (21) Kresse, G.; Furthmüller, J. *Comput. Mater. Sci.* **1996**, *6*, 15.
- (22) Andreoni, W.; Curioni, A. *Parallel Computing* **2000**, *26*, 819.
- (23) Danckwerts, P. V. *Chem. Eng. Sci.* **1979**, *34*, 443.
- (24) Srivastava, R.; Srinivas, D.; Ratnasamy, P. *Microporous Mesoporous Mater.* **2006**, *90*, 314.
- (25) Sayari, A.; Belmabkhout, Y. *J. Am. Chem. Soc.* **2010**, *132*, 6312.
- (26) Chang, A. C. C.; Chuang, S. S. C.; Gray, M.; Soong, Y. *Energy Fuels* **2003**, *17*, 468.
- (27) Couck, S.; Denayer, J. F. M.; Baron, G. V.; Remy, T.; Gascon, J.; Kapteijn, F. *Phys. Chem. Chem. Phys.* **2010**, *12*, 9413.
- (28) Volklinger, C.; Loiseau, T.; Guillou, N.; Ferey, G.; Elkaim, E.; Vimont, A. *Dalton Trans.* **2009**, 2241.
- (29) Nakanaga, T.; Ito, F. *J. Phys. Chem. A* **1999**, *103*, 5440.
- (30) Honda, M.; Fujii, A.; Fujimaki, E.; Ebata, T.; Mikami, N. *J. Phys. Chem. A* **2003**, *107*, 3678.
- (31) Piracha, N. K.; Nakanaga, T. *J. Mol. Struct.* **2002**, *611*, 179.
- (32) Southern, C. A.; Levy, D. H.; Florio, G. M.; Longarte, A.; Zwier, T. S. *J. Phys. Chem. A* **2003**, *107*, 4032.
- (33) Zhang, J.; Zhang, S.; Dong, K.; Zhang, Y.; Shen, Y.; Lv, X. *Chem.—Eur. J.* **2006**, *12*, 4021.
- (34) Rocchia, M.; Garrone, E.; Geobaldo, F.; Boarino, L.; Sailor, M. J. *Phys. Status Solidi A* **2003**, *197*, 365.
- (35) Boutin, A.; Couck, S.; Coudert, F.-X.; Serra-Crespo, P.; Gascon, J.; Kapteijn, F.; Fuchs, A. H.; Denayer, J. F. M. *Microporous Mesoporous Mater.* **2011**, *140*, 108.
- (36) Walker, A. M.; Civalieri, B.; Slater, B.; Mellot-Draznieks, C.; Corà, F.; Zicovich-Wilson, C. M.; Román-Pérez, G.; Soler, J. M.; Gale, J. D. *Angew. Chem., Int. Ed.* **2010**, *41*, 7501.
- (37) Mendt, M.; Jee, B.; Stock, N.; Ahnfeldt, T.; Hartmann, M.; Himsl, D.; Pöppel, A. *J. Phys. Chem. C* **2010**, *114*, 19443.
- (38) Svelle, S.; Tuma, C.; Rozanska, X.; Kerber, T.; Sauer, J. *J. Am. Chem. Soc.* **2009**, *131*, 816.
- (39) Boutin, A.; Couck, S.; Coudert, F.-X.; Serra-Crespo, P.; Gascon, J.; Kapteijn, F.; Fuchs, A. H.; Denayer, J. F. M. *Microporous Mesoporous Mater.* **2010**, In Press.
- (40) Ghoufi, A.; Maurin, G. *J. Phys. Chem. C* **2010**, *114*, 6496.
- (41) Rosenbach, N.; Ghoufi, A.; Deroche, I.; Llewellyn, P. L.; Devic, T.; Bourrelly, S.; Serre, C.; Ferey, G.; Maurin, G. *Phys. Chem. Chem. Phys.* **2010**, *12*, 6428.
- (42) Salles, F.; Jobic, H.; Devic, T.; Llewellyn, P. L.; Serre, C.; Ferey, G.; Maurin, G. *ACS Nano* **2010**, *4*, 143.
- (43) Serre, C.; Bourrelly, S.; Vimont, A.; Ramsahye, N.; Maurin, G.; Llewellyn, P.; Daturi, M.; Filinchuk, Y.; Leynaud, O.; Barnes, P.; Férey, G. *Adv. Mater.* **2007**, *19*, 2246.
- (44) Torrisi, A.; Mellot-Draznieks, C.; Bell, R. G. *J. Chem. Phys.* **132**, 044705.
- (45) Torrisi, A.; Mellot-Draznieks, C.; Bell, R. G. *J. Chem. Phys.* **2009**, *130*, 194703.
- (46) Torrisi, A.; Bell, R. G.; Mellot-Draznieks, C. *Cryst. Growth Des.* **2010**, *10*, 2839.
- (47) Espinosa, E.; Molins, E.; Lecomte, C. *Chem. Phys. Lett.* **1998**, *285*, 170.
- (48) Mata, I.; Alkorta, I.; Molins, E.; Espinosa, E. *Chem.—Eur. J.* **2010**, *16*, 2442.
- (49) Vaidhyanathan, R.; Iremonger, S. S.; Shimizu, G. K. H.; Boyd, P. G.; Alavi, S.; Woo, T. K. *Science* **2010**, *330*, 650.
- (50) Bourrelly, S.; Llewellyn, P. L.; Serre, C.; Millange, F.; Loiseau, T.; Ferey, G. *J. Am. Chem. Soc.* **2005**, *127*, 13519.
- (51) Uemura, K.; Matsuda, R.; Kitagawa, S. *J. Solid State Chem.* **2005**, *178*, 2420.
- (52) Babarao, R.; Jiang, J. *Langmuir* **2008**, *24*, 6270.
- (53) Chaffee, A. L.; Knowles, G. P.; Liang, Z.; Zhang, J.; Xiao, P.; Webley, P. A. *International Journal of Greenhouse Gas Control* **2007**, *1*, 11.
- (54) D'Alessandro, D. M.; Smit, B.; Long, J. R. *Angew. Chem., Int. Ed.* **2010**, *49*, 6058.